

Supporting Information

Controllable mitochondrial aggregation and fusion by a programmable DNA binder

Longyi Zhu,^a Yiting Shen,^a Shengyuan Deng,^c Ying Wan,^{*,b} Jun Luo,^a Yan Su,^b Mingxu You,^d Chunhai Fan,^e and Kewei Ren^{*,a}

^aSchool of chemistry and chemical engineering, Nanjing university of science and technology, Nanjing 210094, China. E-mail: kwren@njust.edu.cn

^bIntelligent microsystem technology and engineering center, School of mechanical engineering, Nanjing university of science and technology, Nanjing 210094, P.R. China. E-mail: wanying@njust.edu.cn.

^cSchool of environmental and biological engineering, Nanjing university of science and technology, Nanjing 210094, P.R. China.

^dDepartment of chemistry, University of massachusetts, Amherst, MA 01003, USA

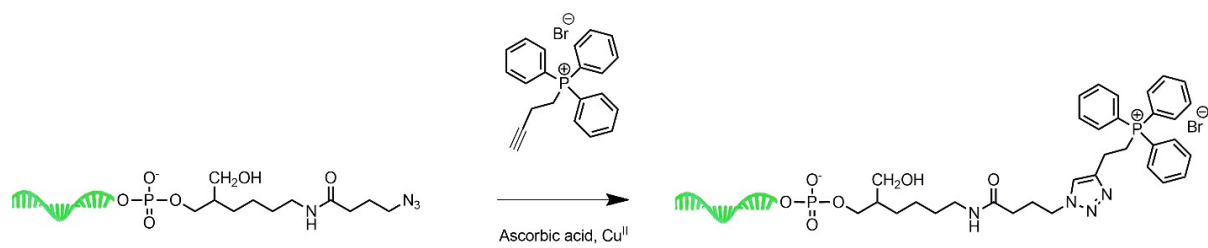
^eSchool of chemistry and chemical engineering, Shanghai jiao tong university, Shanghai 200127, China.

Contents

Table S1	S2
Scheme S1	S3
Supporting Figures S1-S21	S4-S12

Table S1. The binding sequences of primer1 and liner DNA1 are shown in bold. The binding sequences of primer2 and liner DNA2 are shown in bold and italic. The ATP aptamer sequences in SA1 (TAMRA-SA1) and BHQ-SA2 are shown in blue.

Primer1	AATCTGGCTGCGCTTGAA
Ligation DNA1	TGCTTTAGGAAATCTGGCTG
Linear DNA1	P-TCCTAAAGCATGACCTTCCGTTTCCGTAGTTTCAAGCGCAGCCAGATT
Primer-12	AATCTGGCTGCGGAAACG
Linear DNA-12	P-TCCTAAAGCATGACCTTCCGTTTCCGCAGCCAGATT
Linear DNA-36	P-TCCTAAAGCATGACCTTCCGTTTCCGTAGTTTCAAGCGTAGTTTCAAGCGCAGCCAGATT
Linkage DNA	TCCTAAAGCATGACCTTCCGTTTCTTTTTTTTTTTT-Azide
DA	TCCTAAAGCATGACCTTCCGTTTCCGTAGTTTCA
FAM-linkageDNA	TCCTAAAGCATGACCTTCCGTTTCTTTTTTTTTTTT-FAM
FAM-O1	FAM-GAAACGGAAGGTCATGCTTTAGGA
FAM-O2	FAM-CGTAGTTTCAAGCGCAGCCAGATT
Primer2	<i>TTTTGCGGAGGAAGGTTT</i>
Ligation DNA2	AGGAAGGTTTTTTTGGCGGAG
Linear DNA2	P-AAACCTTCCTCCGCAAAAAACCTTCCTCCGCAAAAA <i>ACCTTCCTCCGC</i> <i>AAAA</i>
SA1	<i>ACCTGGGGGAGTAT</i> TTTTTTTTTTTTTTT-Azide
TAMRA-SA1	TAMRA- <i>ACCTGGGGGAGTAT</i> TTTTTTTTTTTTTTT
CSA1	GACGCGTGAGTAGTTTTTTTTTTTTTTT-Azide
TAMRA-CSA1	TAMRA-GACGCGTGAGTAGTTTTTTTTTTTTTTT
BHQ-SA2	<i>TGCGGAGGAAGGT</i> -BHQ2



Scheme S1. Synthetic route to TPP-LDNA.

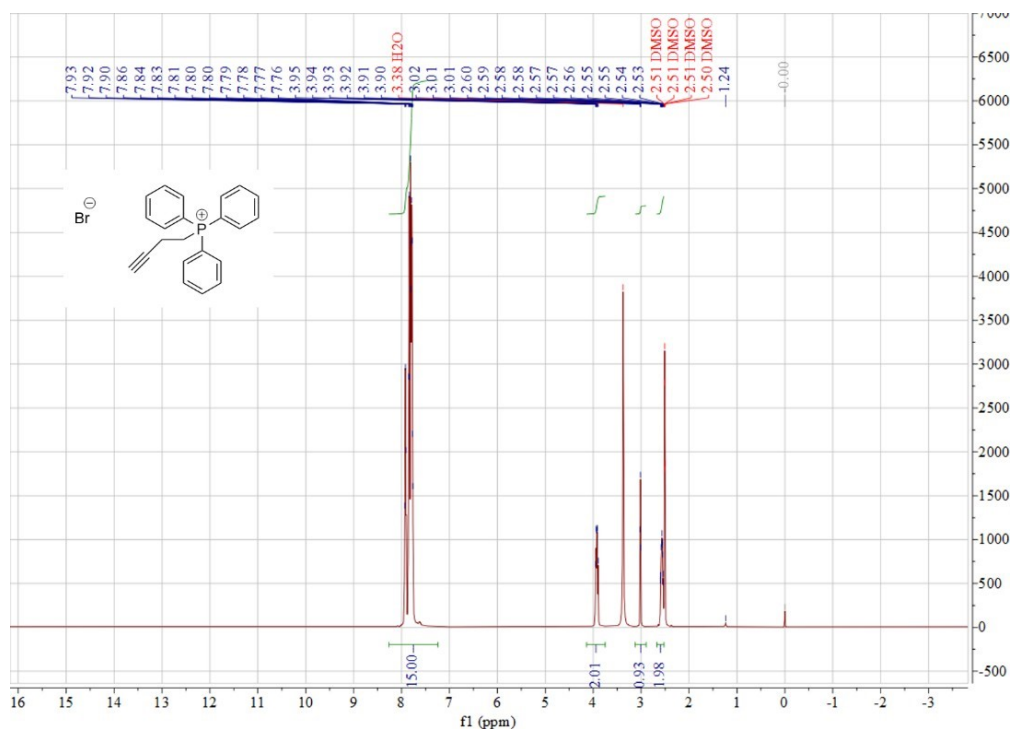


Figure S1. ¹H-NMR spectrum of alkynyl-TPP.

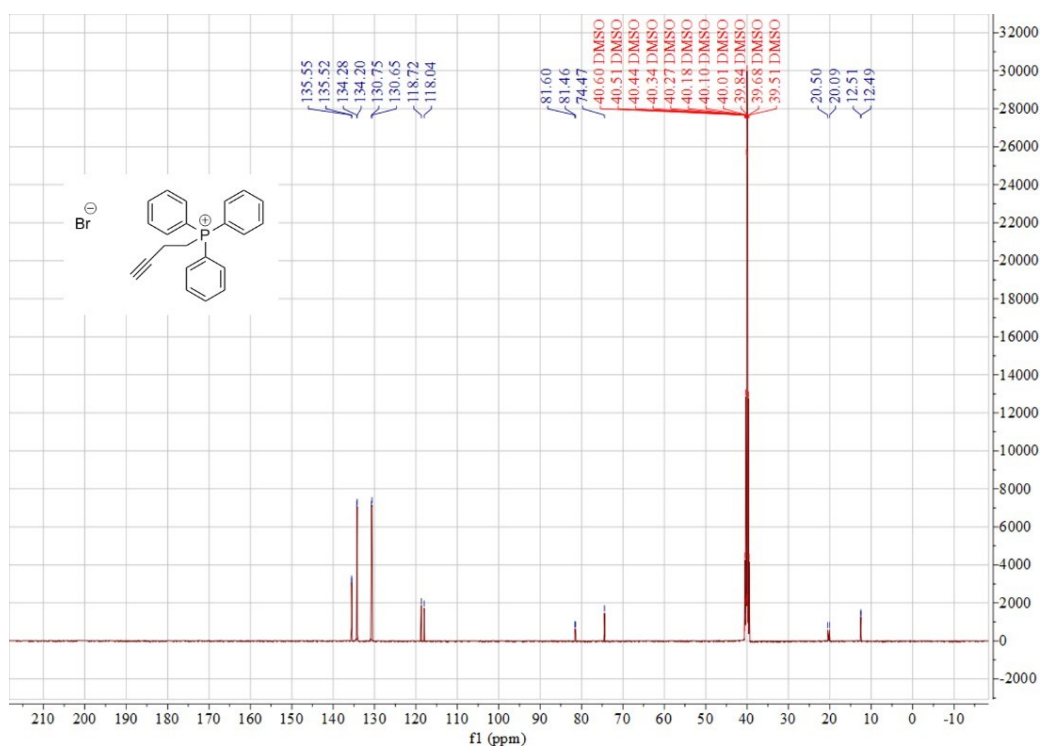


Figure S2. ¹³C-NMR spectrum of alkynyl-TPP.

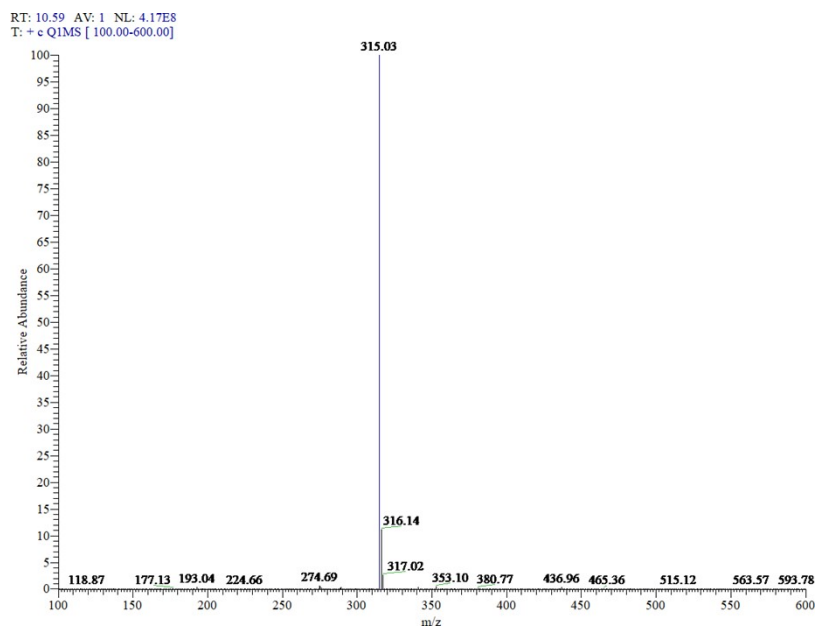


Figure S3. ESI-MS spectrum of alkynyl-TPP cation.

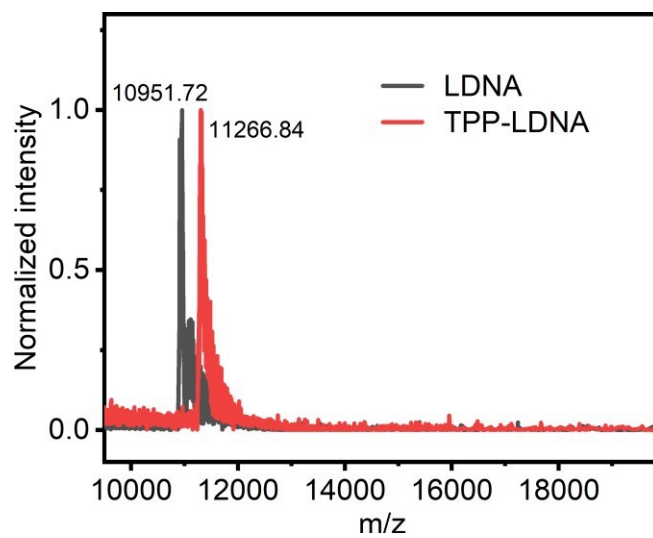


Figure S4. MALDI-TOF MS spectra of LDNA and TPP-LDNA.

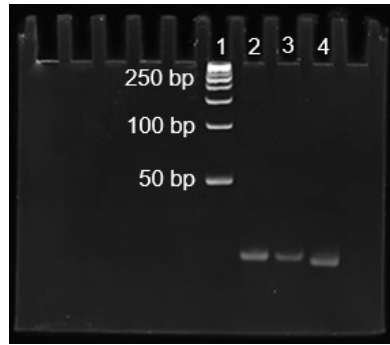


Figure S5. 15 wt% native polyacrylamide gel electrophoresis of TPP-LDNA reaction solution (lane 2) and TPP-LDNA after purification (lane 3) and LDNA (lane 4). The gel was run for 80 min at 100 mV in 1X TBE (Tris-Borate-EDTA) buffer.

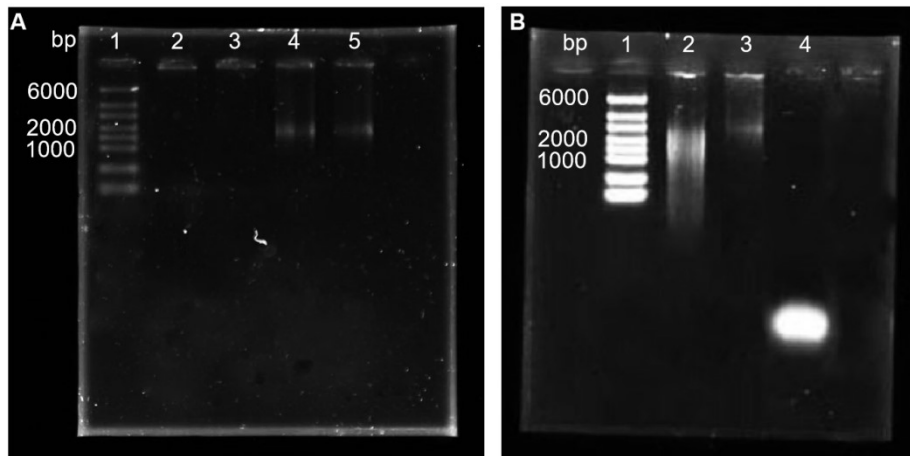


Figure S6. (A) 0.6 wt% agarose gel electrophoresis of DNA chain using 0.05 (2), 0.1 (3), 0.2 (4), 0.4 (5) U/ μ L of Phi29 polymerase. (B) 0.6 wt% agarose gel electrophoresis of DNA chain (2), DNA binder (3), and TPP-LDNA (4). The gel was run for 40 min at 100 mV in 1X TBE (Tris-Borate-EDTA) buffer.

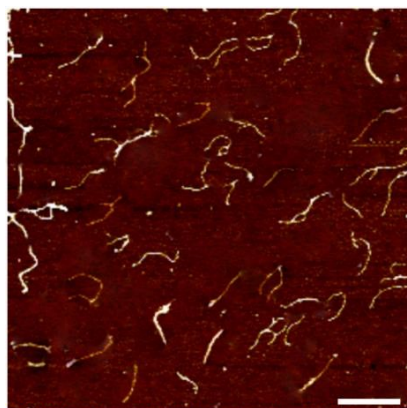


Figure S7. AFM image of DNA binders (5 nM). Multiple threads were observed and found to have an average length of 500 ± 150 nm from a set of 100 features, Scale bar, 600 nm.

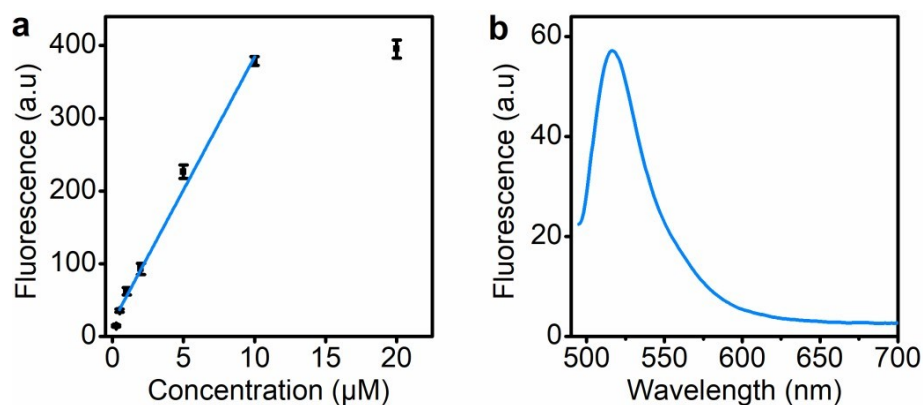


Figure S8. Grafting ratio calculation of TPP-LDNA on the DNA chain. (a) Standard calibration curves for FAM-LDNA at λ_{ex} of 488 nm. The data error bars indicate means \pm SD ($n=3$). (b) Fluorescence spectrum of 1.0 μM F-binder. The concentration of FAM-LDNA strands was calculated as 0.93 μM according to the linear equation.

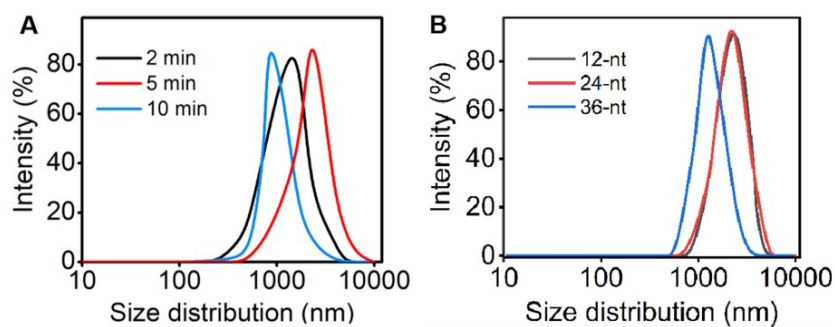


Figure S9. DLS results of (A) mitochondria treated with 1 μM DNA binders with different synthetic time of RCA process, and (B) mitochondria treated with 1 μM DNA binders containing 12-nt (black), 24-nt (red) and 36-nt (blue) interspersed sequences.

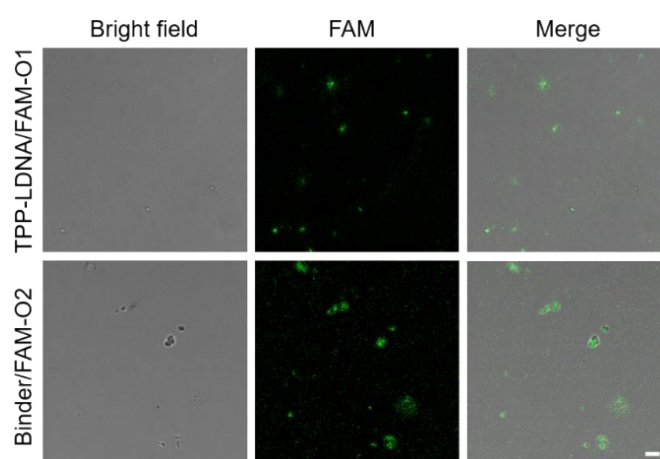


Figure S10. Confocal fluorescence images of extracellular mitochondria treated with 1.0 μM TPP-LDNA/FAM-O1 complex and Binder/FAM-O2 complex. Scale bar: 2 μm .

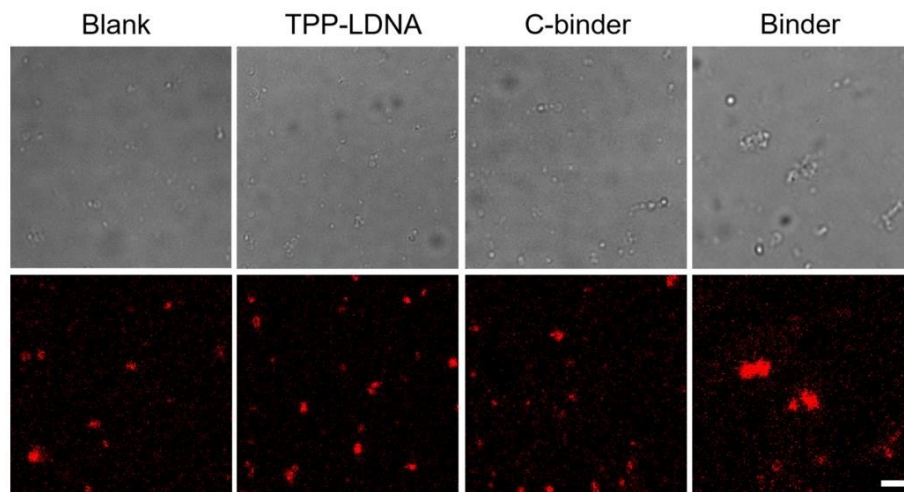


Figure S11. Confocal fluorescence study of extracellular mitochondria (blank) after treated with 1.0 μM TPP-LDNA, C-Binder and DNA binder, respectively. Scale bar: 1 μm .

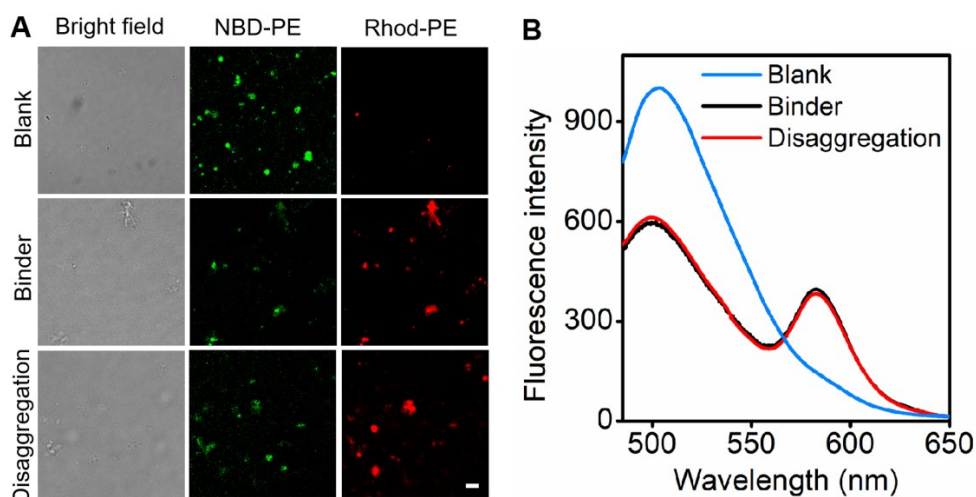


Figure S12. FRET studies of mitochondria fusion by (A) confocal imaging under the excitation wavelength of 488 nm, and (B) fluorescence spectra at an excitation wavelength of 460 nm. Two sets of extracellular mitochondria stained with 2.0 μM of N-(7-nitro-2-1,3-benzoxadiazol-4-yl)-1,2-dipalmitoyl-sn-glycero-3-phosphoethanolamine (NBD-PE) and 2.0 μM of N-(lissamine rhodamine B sulfonyl)-1,2-dipalmitoyl-sn-glycero-3-phosphoethanolamine (Rhod-PE) respectively at 37 $^{\circ}\text{C}$ for 1 h, followed by centrifugation and washing with PBS to remove the excess fluorescence probes. The two resulting mitochondria pellets were dispersed in PBS buffer (pH 7.4) respectively and mixed together. The heterogenous stained mitochondria mixture was treated with (Binder) and without (Blank) 1.0 μM of DNA binder respectively at 37 $^{\circ}\text{C}$ for 15 min. The Binder treated mitochondria mixture was further incubated with 5.0 μM of DA at 37 $^{\circ}\text{C}$ for 30 min (Disaggregation). Finally, confocal imaging and spectra recording was carried out. Scale bar: 2 μm .

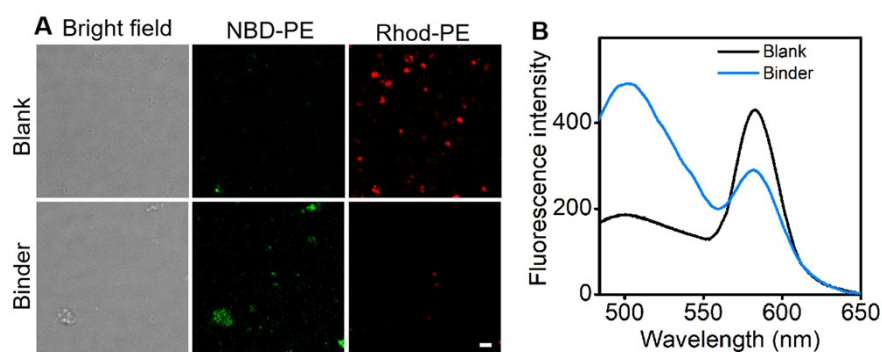


Figure S13. FRET studies of mitochondria fusion by (A) confocal imaging under the excitation wavelength of 488 nm, and (B) fluorescence spectra at an excitation wavelength of 460 nm. One set of extracellular mitochondria was stained with 2.0 μM NBD-PE and 2.0 μM of Rhod-PE at 37 $^{\circ}\text{C}$ for 1 h, followed by centrifugation and washing with PBS to remove the excess fluorescence probes. The resulting mitochondria were dispersed in PBS buffer (pH 7.4) and mixed with the other set of unlabeled extracellular mitochondria. Subsequently the mitochondria mixture was treated with (Binder) and without (Blank) 1.0 μM of DNA binder respectively at 37 $^{\circ}\text{C}$ for 15 min before confocal imaging or spectra recording. Scale bar: 2 μm .

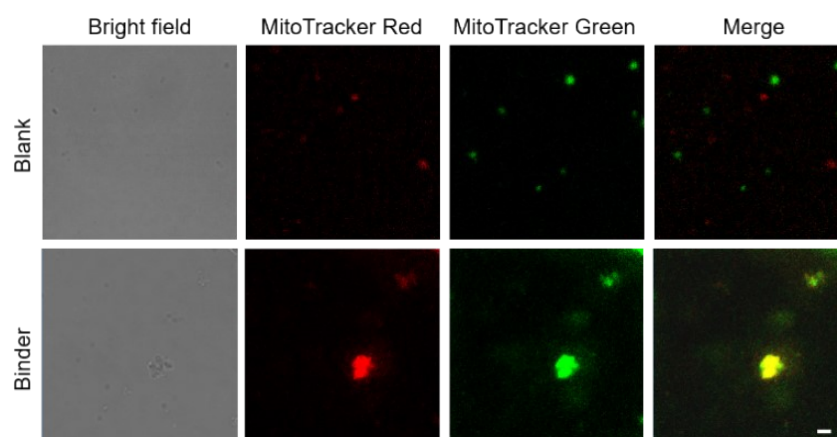


Figure S14. Confocal fluorescence study of two sets of extracellular mitochondria stained with MitoTracker dyes before (Blank) and after treated with 1.0 μM DNA binder (Binder), respectively. Scale bar: 2 μm .

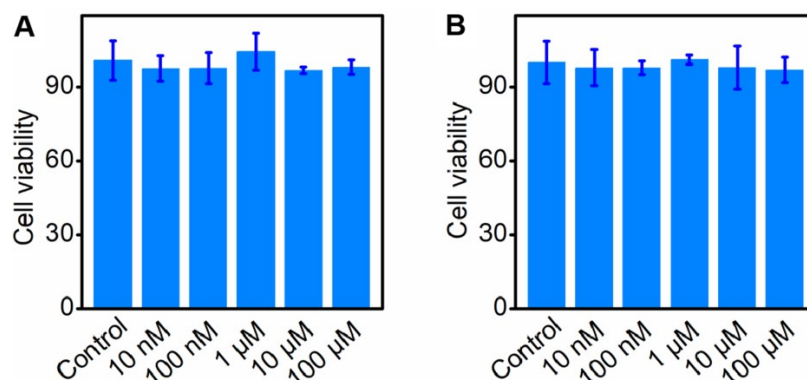


Figure S15. Cytotoxicity of DNA binders. Cell viabilities of (A) 4T1 and (B) SH-SY5Y cells in the absence (Control) and presence of different concentration of DNA binder. The data error bars indicate means \pm SD (n = 3).

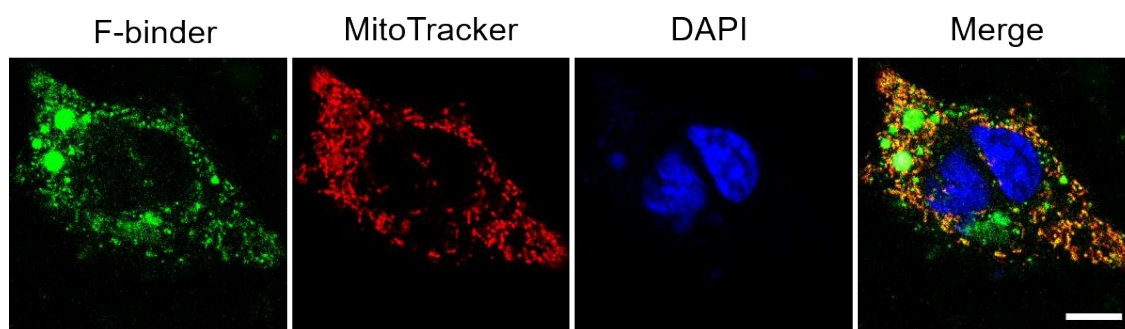


Figure S16. Co-localization study of DNA binders in living cells. Co-staining of 4T1 cells with MitoTracker (red) and DAPI (blue) after incubation with 1.0 μM F-binder (green) for 24 h. Scale bar: 10 μm .

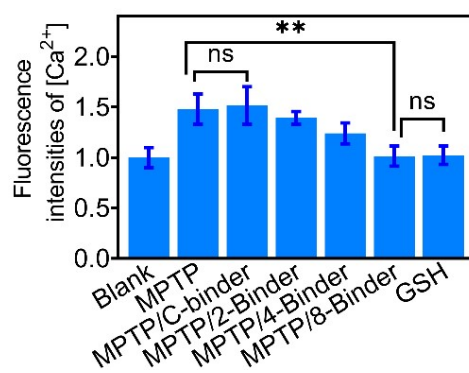


Figure S17. Measurements of intracellular Ca^{2+} levels of different experimental conditions. Blank, SH-SY5Y cells; MPTP, 1 mM MPTP-pretreated SH-SY5Y cells; MPTP/C-binder, 1 mM MPTP-pretreated SH-SY5Y cells with 8 μM C-binder; MPTP/ x -Binder, 1 mM MPTP-pretreated SH-SY5Y cells with x μM DNA binder, $x = 2, 4, 8$; GSH, 5 mM GSH with 1 mM MPTP-pretreated SH-SY5Y cells for 24 h at 37 $^{\circ}\text{C}$. Shown are mean \pm SD. ($n = 3$). ** $P < 0.01$ (two-tailed Student's t -test).

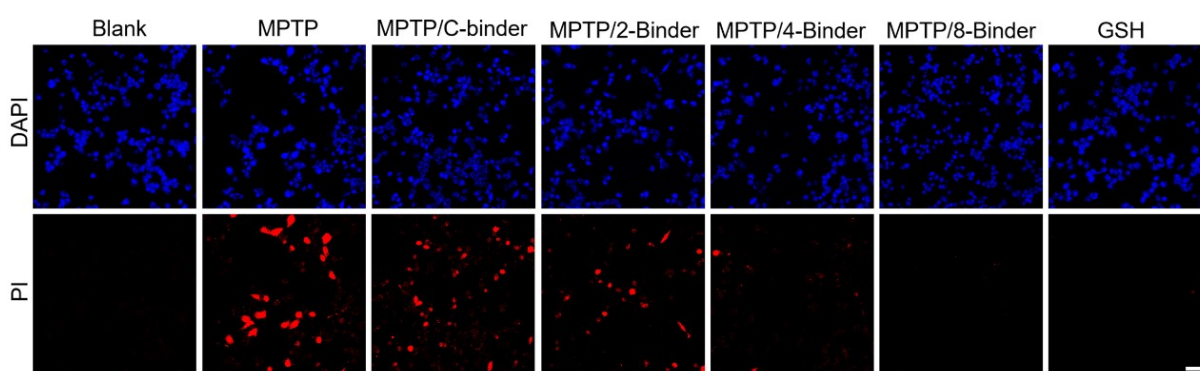


Figure S18. Propidium iodide staining experiments for different experimental conditions. Blank, SH-SY5Y cells; MPTP, 1 mM MPTP-pretreated SH-SY5Y cells; MPTP/C-binder, 1 mM MPTP-pretreated SH-SY5Y cells with 8 μM C-binder; MPTP/ x -Binder, 1 mM MPTP-pretreated SH-SY5Y cells with x μM DNA binder, $x = 2, 4, 8$; GSH, 5 mM GSH with 1 mM MPTP-pretreated SH-SY5Y cells for 24 h at 37 $^{\circ}\text{C}$. Scale bar: 50 μm .

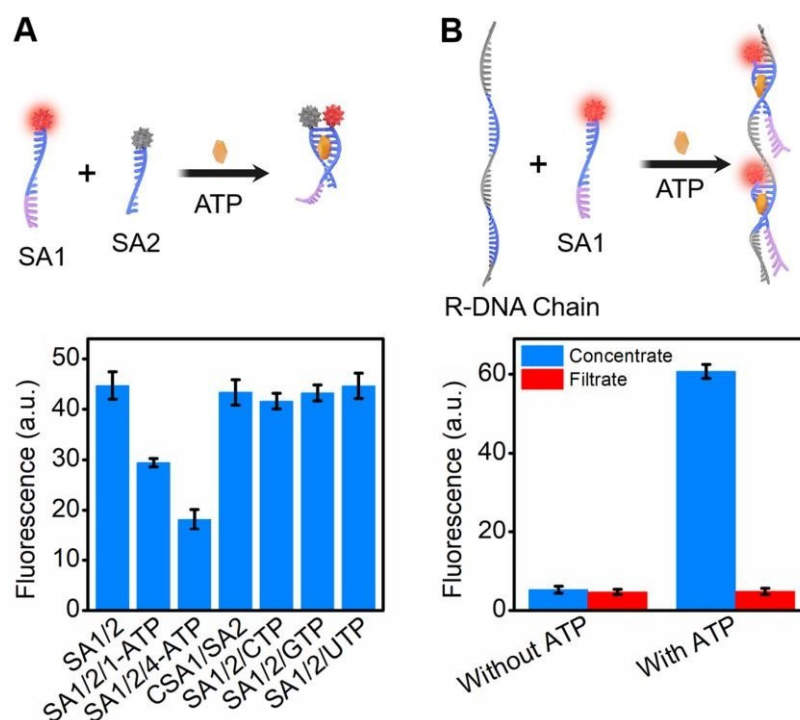


Figure S19. Schematics (upper) and characterization (bottom) of self-assembled ATP-triggered DNA switches and R-DNA binder response. (A) Fluorescence intensities of split aptamer mixture (SA1/2) incubated with 1 mM ATP (SA1/2/1-ATP) and 4 mM ATP (SA1/2/4-ATP). Control experiments were carried out by mixing SA1/2 with 4 mM CTP (SA1/2/CTP), GTP (SA1/2/GTP) and UTP (SA1/2/UTP), as well as mixing random SA1 sequence (CSA1) and SA2 with 4.0 mM ATP (CSA1/SA2). (B) The fluorescence experiment for verification of ATP-triggered responsive DNA binder. 2 μM of TAMRA-SA1 and 2 μM of R-DNA chain were mixed in the presence and absence of 4.0 mM ATP. The resulting mixtures were ultrafiltrated to remove the no-binding TAMRA-SA1 by using PBS as washing agent. When washing with PBS for the third time, the fluorescence intensities of concentrated solution and filtrate were recorded. As shown in Figure S9B, in the presence of ATP, TAMRA-SA1 was immobilized on the R-DNA chain and fluorescence was detected in the concentrated solution, but not in the filtrate. As a control experiment, very weak fluorescence was recorded in both concentrated solution and filtrate in the absence of ATP, indicating that TAMRA-SA1 was washed away without binding with R-DNA chain. The data error bars indicate means \pm SD ($n = 3$). $\lambda_{\text{ex/em}} = 549/580$ nm.

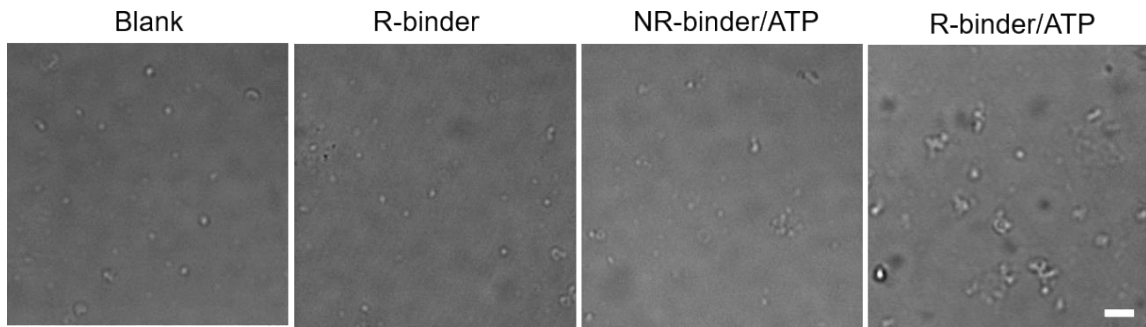


Figure S20. Confocal fluorescence study of extracellular mitochondria aggregation by ATP-triggered DNA binders. Extracellular mitochondria (blank) after incubation with 1.0 μM R-binder in the absence and presence of 2.0 mM ATP, as well as NR-Binder in the presence of 2.0 mM ATP. Scale bar, 10 μm .

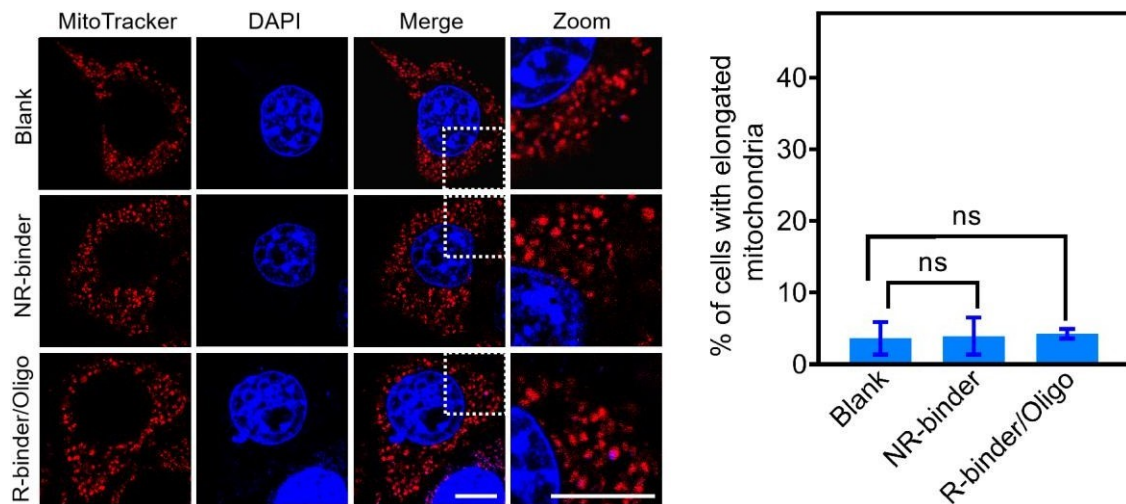


Figure S21. Control study of mitochondria aggregation in living cells. Confocal fluorescence images of 4T1 cells with and without (Blank) 1.0 μM NR-binder, and 1.0 μM NR-binder and 10 μM oligomycin, respectively. The nucleus and mitochondria were staining with DAPI (blue) and mitochondria tracker red (red), respectively. Scale bars, 10 μm . The percentage of cells with elongated mitochondria in these experiments. For each construct, 100 cells were scored in biological triplicate.